Catalysis Today 149 (2010) 91–97

Contents lists available at ScienceDirect

Catalysis Today

journal homepage: www.elsevier.com/locate/cattod

Effect of Li Promoter on titania-supported Rh catalyst for ethanol formation from CO hydrogenation

Adefemi Egbebi [a], Viviane Schwartz [a], Steven H. Overbury [b], James J. Spivey [a,*]

[a] Louisiana State University, Cain Department of Chemical Engineering, Jesse Coates Hall, S. Stadium Drive, Baton Rouge, LA 70803, United States
[b] Oak Ridge National Laboratory, Oakridge, TN 37831, United States

ARTICLE INFO

Article history:
Available online 12 October 2009

Keywords:
Syngas
Ethanol
Rhodium catalyst
Lithium promoter
Titania support

ABSTRACT

The addition of 0.10 wt% Li to Rh/TiO_2 more than doubled the CO conversion for CO hydrogenation while increasing ethanol selectivity. The addition of Li also increases formation of C_2 oxygenates at the expense of C_1 species, methanol and methane. This is attributed to enhanced dispersion of Rh by Li that appears to reduce dissociation of CO, which previous studies have shown requires large ensembles of Rh atoms on the surface. Li promotion appears to increase the associatively adsorbed CO, allowing for increased H_2 chemisorption on the surface compared to the dissociative adsorption of the same number of CO atoms. This increases selectivity to ethanol compared to the unpromoted catalysts. CO-TPD shows more reactive adsorbed CO species on the Li-promoted catalyst. FTIR results suggest that Li promotion alters CO bonding at bridged or interfacial sites and its effect is more structural than electronic.

1. Introduction

It is well known that rhodium-based catalysts are active for the formation of C_2 oxygenates from the hydrogenation of CO [1–6]. Thermodynamic analysis shows that ethanol selectivity is very low unless the formation of methane can be minimized kinetically [7]. The use of alkali promoters has been shown to shift selectivities towards ethanol and other C_2 oxygenates [7–9].

These alkali promoters enhance oxygenate formation by suppressing the hydrogenation activity of Rh (and other group VIII metals) [9]. However the formation of C_2+ oxygenates also requires that intermediates/precursors be hydrogenated. Alkali promotion is therefore only effective if the hydrogenation suppression decreases the formation of methane more than that of C_2+ oxygenates [10]. Chuang et al. [9] tested a series of alkali promoters on Rh/TiO_2 and reported that their ability to enhance selectivity to oxygenates increased in the order: unpromoted < Li < K = Cs while overall CO conversion decreases in the order: unpromoted > Li > K > Cs. Thus in this study, CO conversion is correlated inversely with oxygenate selectivity.

Alkalis may promote oxygenate formation by either changing the electronic state of Rh, causing a change in the surface population of CO species and therefore the proportion of sites available for hydrogenation of surface C species [11]; or blocking of Rh surface sites, thereby inhibiting reaction steps like CO dissociation that requires large ensembles of atoms [12,13]. Regardless of the specific mechanism of promotion, Li generally suppresses methanation/hydrocarbon formation and increases selectivity to C_2+ oxygenates while reducing CO conversion [4,8,9,11].

Most previous work on supported Rh has been on SiO_2 supports [1,14–16], with relatively less literature on Al_2O_3-supported Rh [17,18] and very little on Rh/TiO_2 [9]. Both Al_2O_3 and TiO_2 supports have been reported to have a high density of surface hydroxyls, which provide anchors for catalysts precursors on the surface of the metal oxide [19–21]. Therefore, the hydroxyl population affects the particle size of the supported metal while the hydroxyl density may affect the interactions between neighboring cations or atoms of the supported metals [17]. Here, we use TiO_2 as the support because of it high surface density of reactive hydroxyls (relative to SiO_2) which allows the formation of a close-packed monolayer of the supported metal [17,21]. Rh/TiO_2 has also been found to be more active for CO decomposition and hydrogenation than Rh/SiO_2 or Rh/Al_2O_3 [22], leading to higher activity for methanation and water gas shift. Li promotion can be used to modify the properties of Rh/TiO_2 to increase selectivity towards C_2+ oxygenates in general, and ethanol in particular, while minimizing methane selectivity.

In this work, we have studied Rh/TiO_2 and $Rh–Li/TiO_2$, catalysts with the purpose of examining the effect of Li promotion of Rh/TiO_2 on ethanol (or C_2+ oxygenates) production from synthesis gas.

* Corresponding author. Tel.: +1 225 578 3690; fax: +1 225 578 1476.
E-mail address: jjspivey@lsu.edu (J.J. Spivey).

0920-5861/$ – see front matter © 2009 Elsevier B.V. All rights reserved.
doi:10.1016/j.cattod.2009.07.104

2. Experimental

2.1. Catalyst preparation

1% Rh/TiO_2 and 1% Rh–0.1% Li/TiO_2 (yielding a Li:Rh molar ratio of about 1/1), catalysts were prepared using conventional incipient wetness impregnation. Aqueous solutions of $Rh(NO_3)_3$ and $LiNO_3$ were co-impregnated on TiO_2 (Degussa Aerolyst 7710 [based on P25], ~50 m^2/g), dried overnight at 110 °C and calcined under air for 4 h at 500 °C.

2.2. Catalyst activity test

Reaction tests at differential CO conversions were carried out in a 1/4″ glass-lined stainless steel fixed bed micro-reactor system at 260 and 270 °C and total pressure of 20 bar. Prior to reaction tests the catalyst was reduced in situ for 2 h in 75% H_2/25% He mixture. CO hydrogenation ($H_2/CO = 2$) reactions were run at GHSVs of 52800 scc $(h\ g_{cat})^{-1}$. For each run the syngas feed was diluted with He to reduce heat effects within the bed and to ensure that the conversion is low enough to keep the oxygenated products in vapor state for online GC/MS analysis. The total inlet flow rate was 220 scc/min, consisting of 80 scc/min H_2, 40 scc/min CO and 100 scc/min He. Reactions are allowed to run for at least 1.5 h to attain steady state before samples are injected into the GC. Analysis of products was done using an online Agilent GC/MS system (Agilent Technologies 6890N/5975B) equipped with a thermal conductivity detector (TCD). The line from the reactor exit to the sampling valves is heat traced to prevent products from condensing upstream of the GC/MS. The sampling valves are placed in an isothermal oven and maintained at a temperature of 250 °C. Oxygenates and C_2–C_4 hydrocarbon analysis was done using the mass selective detector (MSD) while hydrogen, CO, CO_2 and CH_4 were analyzed by TCD.

2.3. Temperature programmed reduction (TPR)

250 mg of the catalyst sample was placed in the center of the reactor tube and held in place by the two quartz wool plugs, degassed with He flow at 120 °C for 30 min to remove moisture that might be on the catalysts during storage and allowed to cool to room temperature under He flow. The sample is then exposed to 100 scc/min flow of 10% H_2/Ar gas mixture, as the reactor temperature is ramped at 5 °C/min from room temperature to 500 °C. TCD signal corresponding to H_2 consumption is then recorded as a function of temperature.

2.4. Temperature programmed desorption (TPD)

The catalyst sample was pre-reduced in 100 scc/min of H_2 flow at 350 °C for 2 h and flow switched to He while the sample is allowed to cool to room temperature. The chemisorbing gas, CO, was then allowed to flow over the sample for 1 h at room temperature. Prior to the desorption step, the system is flushed with He for 2 h to remove physisorbed and gas phase CO. Still under He flow, the temperature was linearly ramped from room temperature to 500 °C at 5 °C/min. A quadrupole mass spectrometer (QMS) at the exit of the reactor was used to continuously monitor CO ($m/z = 28$), CO_2 (44) and H_2 (2) as a function of temperature.

2.5. FTIR

The FTIR measurements were made on a Thermo Electron Nexus 670 spectrometer using a MCT detector. A diffuse reflectance infra-red Fourier transform spectroscopy (DRIFTS) cell was obtained from Pike Technologies (DiffusIR) and features a small (approximately 6 ml) reaction volume capable of temperature control from room temperature to 900 °C and operation at atmospheric pressure. In a typical experiment, about 50 mg of Rh-based catalysts were inserted into the DRIFTS cell and reduced under 4% H_2/He at a temperature of 350 °C prior to each experiment. In most of the cases, the cell was flushed with He at 350 °C and then the temperature was lowered to the reaction temperature. A background spectrum was first taken in He and difference spectra were obtained by subtracting the background from the subsequent spectra reported. A manifold of valves was used to switch gases through the DRIFTS cell. Spectra were typically recorded at 4 cm^{-1} resolution and could be recorded every 5 s.

3. Results and discussion

The measured composition (Table 1) is close to the target composition for both catalysts. X-ray diffraction patterns of the catalysts shows only peaks consistent with TiO_2 phases of rutile and anatase. No Rh diffraction pattern is detected as expected for an Rh loading of ~1%. The XRD patterns of Rh/TiO_2 and $Rh–Li/TiO_2$ exactly overlap that of a blank titania support, indicating that the Rh is undetectable by XRD. Inability to detect the Rh may be due to its high dispersion [1] (presumably as an oxide) or its low content.

3.1. Reaction tests

Table 2 shows the selectivity of products for the CO hydrogenation reaction at 260 and 270 °C on both catalysts. The major products formed are methane, acetaldehyde, ethanol, methanol, some C_2–C_3 hydrocarbons along with trace amounts of *n*-propanol and *n*-butanol. The small amount of CO_2 is presumably formed by the WGS reaction. The selectivity and activity largely depend on Li promotion, although there are slight changes in selectivity patterns with temperature, even in the small temperature range explored. The CO conversion increases with temperature, as expected. On both catalysts, increasing the reaction temperature from 260 to 270 °C reduces the total oxygenates, C_2+ oxygenates and ethanol selectivities, while increasing methane formation.

Table 1
Measured composition of the catalysts.

Catalyst	Metal	Composition[a] (wt%)	BET surface area (m^2/g)
Rh/TiO_2	Rh	0.90	45
$Rh–Li/TiO_2$	Rh Li	1.16 0.09	43

[a] Measured with inductively coupled plasma optical emission spectroscopy (ICP-OES).

Table 2
Products selectivity (% carbon efficiency) for CO hydrogenation over promoted Rh/TiO_2 catalysts (reaction conditions: 20 bar, 52,800 scc/h-gcat, $H_2/CO = 2/1$).

	260 °C		270 °C	
	Rh/TiO_2	$Rh–Li/TiO_2$	Rh/TiO_2	$Rh–Li/TiO_2$
Methanol	6.8	3.7	5.5	2.8
Acetaldehyde	8.4	15	9.2	15
Ethanol	12	23	10	17
Methane	58	46	62	55
CO_2	2.5	2.4	2.4	2.0
C_2+ hydrocarbons	8.6	3.6	7.1	4.4
Total oxygenates[a]	30	47	28	38
EtOH/total oxygenates	0.40	0.49	0.37	0.43
$EtOH/CH_4$	0.2	0.50	0.17	0.30
Conversion, mol.% C	0.8	2.0	1.0	2.5

[a] Sum of oxygen containing products, excluding CO and CO_2.

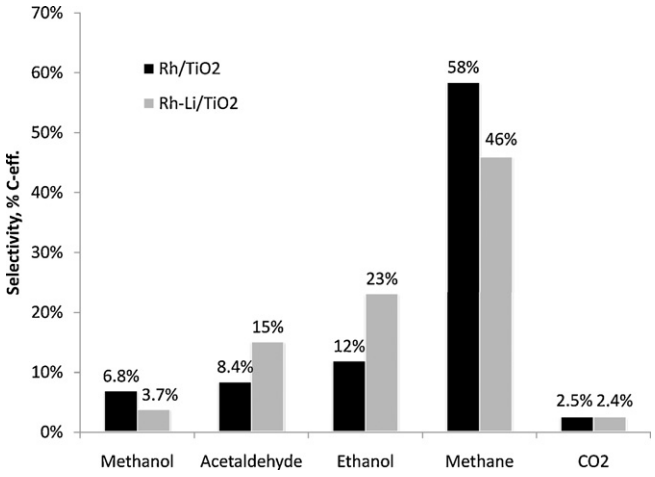

Fig. 1. Products selectivity (% carbon efficiency) for CO hydrogenation over Rh/TiO_2 versus $Rh–Li/TiO_2$ catalysts (reaction conditions: 260 °C, 20 bar, 52,800 scc/h-gcat, $H_2/CO = 2/1$).

Unpromoted Rh/TiO_2 gave higher methane selectivity of 58% at 260 °C than Li-promoted Rh/TiO_2, while selectivities to methanol, ethanol and acetaldehyde are 6.8%, 12% and 8.4% respectively. High methane selectivity suggests significantly more CO dissociation than CO insertion on unpromoted Rh/TiO_2, compared to the Li-promoted catalysts. Higher total selectivity of C_1 species (methanol and methane) on Rh/TiO_2 suggests that the catalyst has a low CO insertion activity but sufficient hydrogenation activity to hydrogenate C_1 intermediates to both methane and methanol.

On $Rh–Li/TiO_2$ at 260 °C, C_2+ oxygenate selectivity is nearly twice that of Rh/TiO_2 (38% versus 20.4%) while methane selectivity decreases from 58% to 46% with Li promotion (Fig. 1). On $Rh–Li/TiO_2$, ethanol is the most abundant oxygenated product and its selectivity (23%) is twice that of the unpromoted catalyst (12%). The C_2+ oxygenated species are produced at the expense of C_1 species (methanol and methane). This can be attributed to the moderating effect of Li on the CO dissociation ability of the Rh/TiO_2. Li promotion also increases the total CO conversion from 0.8% to 2.0% at 260 °C, and from 1.0 to 2.5% at 270 °C. This enhancement of activity on Li (or alkali) promotion is unexpected because the opposite effect is typically reported in literature [8,9,12]. The selectivities to oxygenates decrease with increasing temperature on both catalysts, while that of methane increases. This suggests increased CO dissociation and hydrogenation at higher temperatures.

3.2. CO-TPD

The desorption profiles of CO ($m/z = 28$) from both catalysts (Fig. 2) show that the associative desorption of CO takes place at the same temperature (~92 °C) on both catalysts, suggesting comparable strength of interaction of CO with both surfaces. This further suggests a weak electronic effect of the Li because a much stronger effect would alter the strength of the Rh–CO bonds thereby shifting CO-TPD peak to a higher temperature. The larger CO peak on $Rh–Li/TiO_2$ suggests a higher population of associated CO species on $Rh–Li/TiO_2$, which may be due to more exposed Rh surface for CO adsorption or to less CO dissociation on the $Rh–Li/TiO_2$ catalyst.

Both CO_2 and H_2 were monitored during the CO-TPD experiment, and results are shown in Fig. 3. First, CO_2 is observed at both ~90 °C on both catalysts, and at 280 °C ($Rh–Li/TiO_2$) and at 300 °C (Rh/TiO_2). The low-temperature peak at ~90 °C is at the same temperature at which CO desorbs associatively on both catalysts (Fig. 2). The formation of CO_2 at this temperature, without the

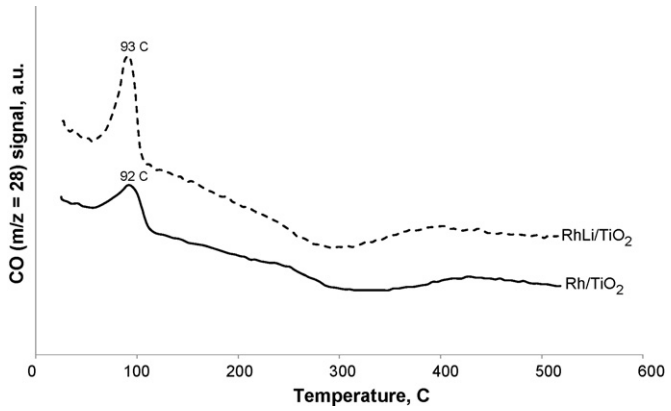

Fig. 2. Desorption profiles of CO from CO-TPD of the unpromoted and the Li-promoted Rh/TiO_2 catalysts, following continuous CO adsorption at room temperature. Curves are offset but on the same intensity scale.

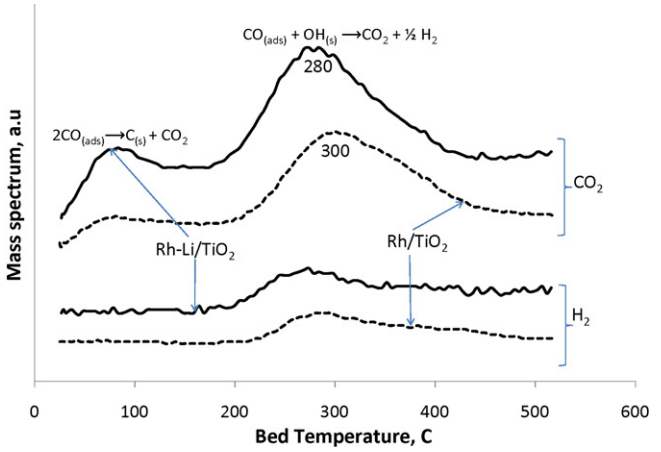

Fig. 3. CO_2 and H_2 desorption from CO-TPD of Rh/TiO_2 and $Rh–Li/TiO_2$ catalysts, following continuous CO adsorption at room temperature.

accompanying formation of H_2, has been attributed to the Bouduard reaction on 0.5% Rh/TiO_2 [22]

$$2CO_{(ad)} \rightarrow C_{(s)} + CO_2 \quad (1)$$

The results here agree with this earlier work [22]. This, combined with the associative desorption of CO at this same temperature, show that CO is adsorbed in two different modes on both catalysts. The fact that (a) CO desorbs associatively, and (b) reacts to form CO_2 at the same temperature suggests that there are two modes of adsorption with similar strengths of interaction with the surface, at least as measured by the temperature at which CO either reacts or desorbs. However, these two modes must be chemically different, since they lead to two different products: desorbed CO in one case and CO_2 in the other. Furthermore, the larger CO peak in Fig. 2 for the $Rh–Li/TiO_2$ catalyst coupled with a greater area under the ~90 °C CO_2 desorption peak in Fig. 3 for $Rh–Li/TiO_2$ corresponds to a greater amount of CO adsorbed on this catalyst, though the modes of adsorption appear to be the same as those on Rh/TiO_2.

Fig. 3 also shows a high-temperature CO_2 desorption peak on each catalyst, with a corresponding H_2 peak. This has been observed on Al_2O_3 and TiO_2 supported Rh catalysts [22] where the CO_2 is said to be formed by the reaction of surface hydroxyl groups with CO species strongly adsorbed to metallic surface:

$$CO_{(ad)} + OH_{(s)} \rightarrow CO_2 + (1/2)H_2 \quad (2)$$

The high-temperature CO_2 peak on $Rh–Li/TiO_2$ is positioned at 280 °C, which is 20 °C lower than that on Rh/TiO_2 (at 300 °C),

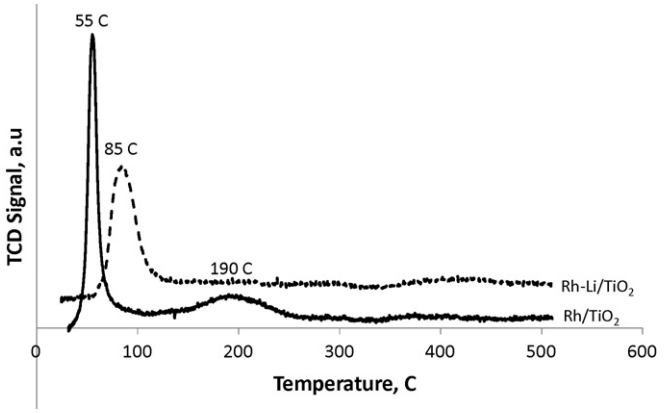

Fig. 4. TPR profiles of the Rh/TiO, and Rh–Li/TiO_2 catalysts. TPR conditions: 5 °C/min heating rate; room temperature to 500 °C; 10% H_2/Ar, 50 scc/min; sample weight, 0.25 gcat.

suggesting that this more strongly adsorbed CO is slightly more reactive on Rh–Li/TiO_2. This is consistent with higher activity observed on the Li-promoted catalysts for CO hydrogenation (Table 2).

3.3. TPR

The TPR profiles of the two catalysts are shown in Fig. 4. Rh/TiO_2 shows two reduction peaks while a single peak is observed for Rh–Li/TiO_2. The low-temperature peak can be attributed to the reduction of surface Rh oxide species and the smaller high-temperature peak for the reduction of bulk Rh species [5,23]. The position of the low-temperature peak shifts from 55 (Rh/TiO_2) to 85 °C (Rh–Li/TiO_2). The shift in peak position with the addition of Li promoter is indicative of decreased reducibility of Rh as a result of the interaction between Rh and Li on the surface. Such interactions can be in the form of surface alloys, leading to shifts in reduction temperatures to an intermediate value between those of the components of the alloy (Li would generally not reduce below 500 °C [5]).

There is a small high-temperature peak for Rh/TiO_2 at 190 °C, corresponding to the reduction of bulk Rh [5,24]. The absence of a bulk Rh peak on Rh–Li/TiO_2 suggests that there is no reducible bulk Rh on the catalyst. The relative areas of the surface and bulk Rh peaks (0.7 for Rh/TiO_2 and 1.0 for Rh–Li/TiO_2) can be used as an indication of relative Rh dispersion. The unexpected increase in CO conversion (Table 2) with Li promotion can therefore be explained by an increase in amount of exposed Rh surface area.

TEM images (Fig. 5a and b) taken at ORNL confirm that the crystallite size of Rh is slightly smaller on the Li-promoted sample than on the unpromoted catalyst. The corresponding Rh particle size distribution from the images are depicted in Fig. 5c, showing that Rh is normally distributed with a mean particle size of Rh on Rh/TiO_2 and Rh–Li/TiO_2 as ~1 and ~1.5 nm respectively.

3.4. FTIR

Fig. 6 shows FTIR spectra while flowing CO over pre-reduced Rh/TiO_2 at variable temperatures and atmospheric pressure.

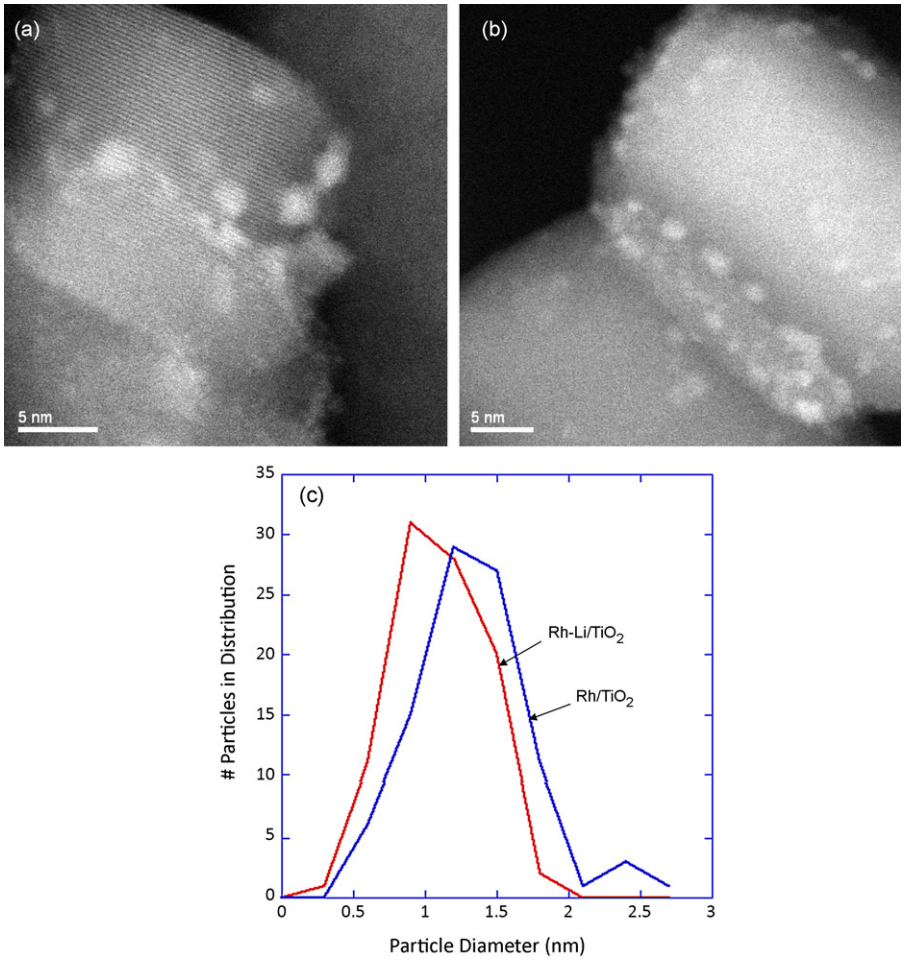

Fig. 5. TEM images of (a) Rh/TiO and (b) Rh–Li/TiO_2 catalysts and (c) corresponding particle size distribution of Rh particles.

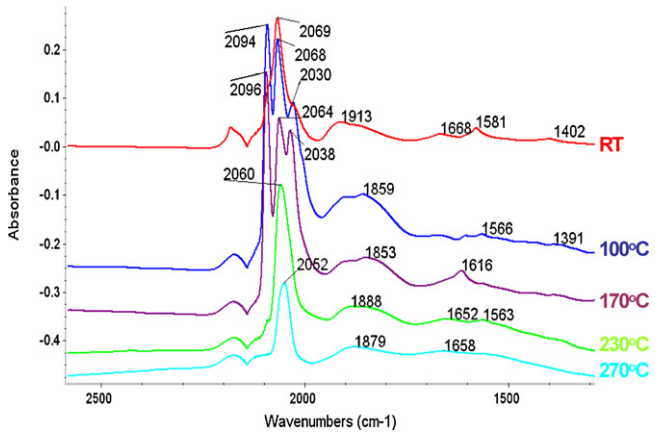

Fig. 6. FTIR spectra during CO adsorption on Rh/TiO_2 at variable temperature.

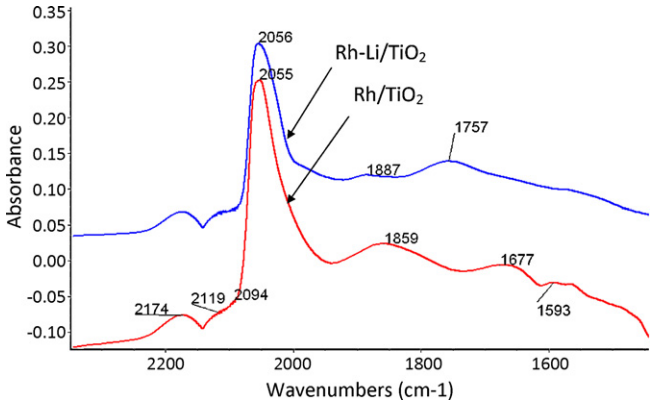

Fig. 7. Comparison of the FTIR spectra for CO adsorption at 270 °C over the pre-reduced Rh/TiO_2 and $Rh–Li/TiO_2$.

Besides the doublet-bands characteristic of phase CO between 2180 and 2120 cm^{-1}, bands characteristic of three adsorption states of CO can be identified: gem-dicarbonyl $Rh^I(CO)_2$, linearly bonded CO on Rh^0, and bridge-bonded CO on Rh^0. The features at 2096 and 2030 cm^{-1} can be attributed to the symmetric and asymmetric carbonyl stretching frequencies of $Rh^I(CO)_2$ [25,26]. These features are visible as shoulders at room temperature where the spectrum is dominated by linear CO. The gem-dicarbonyl features persist at 100 and 170 °C. Interestingly, the gem-dicarbonyl seems to be absent at reaction temperatures (270 °C). Therefore, pre-treatment in H_2 at 350 °C does not completely remove all of the oxidized Rh^I, whereas exposure to CO at 270 °C is sufficient to remove the remaining Rh^I, the sites for the gem-dicarbonyl. FTIR studies by Basu et al. [25] have shown changes of oxidation state of Rh metal supported on Al_2O_3 and SiO_2 following adsorption of CO. Basu et al. propose that chemisorption-induced structural modifications of supported metal aggregates can be expected in such systems and surface hydroxyl groups can be involved in the structural rearrangement of the metal aggregates. FTIR is evidently a sensitive technique for monitoring changes of oxidation state of Rh.

The vibrational frequency at 2048–2069 cm^{-1} is attributed to linearly bonded CO. There is a general trend of shifting the linearly adsorbed CO to lower wave numbers as the temperature is increased and after prolonged reaction. This shift could be due to decreasing coverage. In addition to the linearly bonded CO on Rh^0, the presence of a broad band around 1870 cm^{-1} indicates the presence of bridge-bonded CO on Rh^0 at reaction temperatures. The band shape of bridge-bonded CO on reduced Rh suggests the presence of two components at around 1913 and 1890 cm^{-1}. These two bands have been ascribed to CO adsorption on two Rh crystalline faces, such as Rh(1 0 0) and Rh(1 1 1) [27]. This feature becomes broader with higher temperature and, as described below, is sensitive to Li promotion.

CO adsorption at variable temperatures was also carried out on the Li-promoted Rh/TiO_2 and gave results similar to Fig. 6. This catalyst also showed the presence of the gem-dicarbonyl at room temperature, and detectable gem-dicarbonyl persisted to higher temperatures than for the unpromoted catalysts. Fig. 7 shows a comparison between unpromoted Rh/TiO_2 and $Rh–Li/TiO_2$ catalysts upon CO adsorption at reaction temperatures (270 °C). There is no indication of gem-dicarbonyl species in either case and the linearly bond CO lies at about the same frequency. Contrary to what has been suggested [11,28], the invariance of the linear CO frequency indicates that the promoter is not altering the electronic structure of Rh. At this temperature, the major difference seems to lie in the bridge-bonded feature. The broad feature located between 1859 and 1887 cm^{-1} is more intense in the case of unpromoted Rh while the feature seems to be nearly absent in the promoted catalyst. The weaker intensity of the bridge-bonded feature for the unpromoted catalyst may be tentatively explained by blocking of some of the bridged CO adsorption sited on the corresponding Rh crystalline face. A third more pronounced peak is observed on the Li-promoted catalyst at around 1750 cm^{-1}, which might be too low to be attributable to CO bridge-bonded to several Rh atoms via carbon atom alone. Bridging sites at 1725 and 1696 cm^{-1} at the metal/oxide interface have been observed previously and were assigned to an adsorption state in which the C atom in each CO molecule is bonded to the metal and the O atom bonded to a Ti^{3+} cation [29]. Here, we can speculate that the Li promoter might be the cation site.

In order to further examine the role of the Li promoter during the hydrogenation of CO, FTIR was carried out under the reaction mixture and at the reaction temperature of 270 °C and atmospheric pressure. For this experiment the gas was abruptly switched from a mixture of H_2 and He at 270 °C to a mixture of 2:1 H_2/CO while continuously recording the FTIR spectra. After no changes were observed on the spectra (typically 9 min), the gas stream was switched back to a reducing atmosphere of H_2 and He with continued FTIR monitoring. The FTIR thus provided a continuous record of the changes on the surface through both switches. Fig. 8a and b depict the spectra recorded at about 50 s after each switch.

The spectrum obtained under reaction conditions in Fig. 8a shows only a subtle change in the CO stretching region compared to the CO adsorption experiments in Fig. 7. The presence of adsorbed hydrogen lowers slightly the frequency of the linearly adsorbed CO to 2030 cm^{-1} in the Li-promoted case. This shift might be attributed to hydrogen interactions in a $Rh(CO)H_2$ complex as described previously [30]. Differences between the Li-promoted and the unpromoted catalyst, noted above for CO adsorption, persist in the presence of the reaction mixture and after the switch back to H_2 (Fig. 8b). Continued monitoring after the switch to H_2 indicates that the linear CO reacts more rapidly than the bridged CO.

Other FTIR features in Fig. 8 reveal the nature of the products and intermediates of the CO hydrogenation reaction. Methane formation is clearly evident in Fig. 8a, revealed by the spectroscopic features related to gas phase methane (sharp band at 3016 cm^{-1}) and adsorbed water (broad band below 3500 cm^{-1} and a stronger band around 1616 cm^{-1}). Both methane and water were more clearly noticeable on the unpromoted catalyst. The spectroscopic observation agrees with the reactivity results in which methane formation is higher for the unpromoted Rh catalyst. The band at around 3670 cm^{-1} is assigned to isolated surface hydroxy

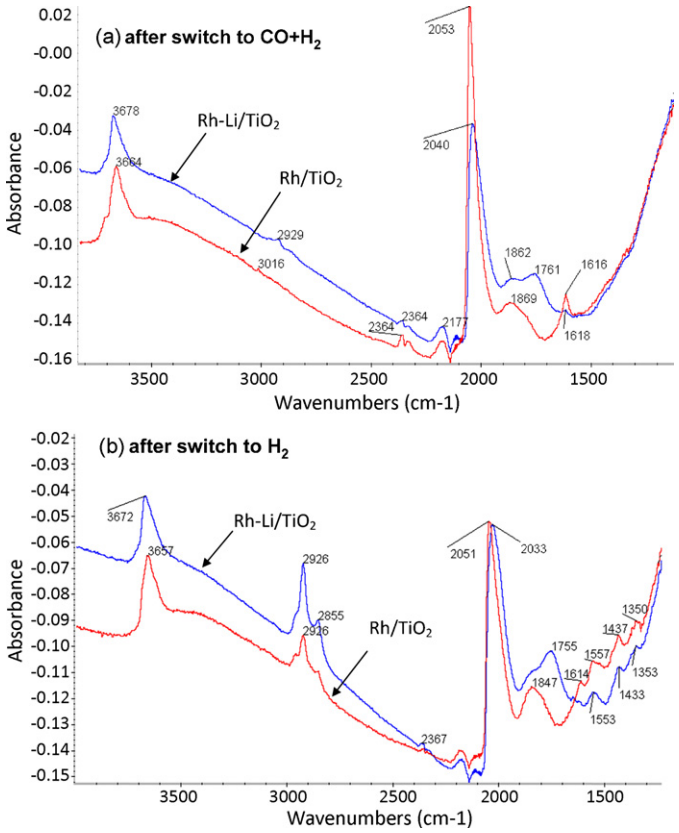

Fig. 8. FTIR spectra recorded during gas switches in which H_2 flow was switched to a mixture of CO + H_2 and then back to H_2. The spectra were recorded about 50 s after each switch.

groups on the titania support that are perturbed under the presence of adsorbed CO species. Fig. 8b clearly shows the presence of three peaks at 2963, 2926 and 2860 cm^{-1} that can be ascribed to C–H stretching vibrations of saturated alkyl groups [29]. The presence of bands around 2960 and 2920 cm^{-1} corresponds to the asymmetric CH_3 and CH_2 vibrations, whereas the band at 2860 cm^{-1} corresponds to the symmetric mode [31]. Peaks at 1533 and 1444 cm^{-1} are assigned to adsorbed carboxylate anions on the titania surface [29] and to CH_3O and C_2H_5O species attached to metal sites [32] These bands in conjunction with the C–H stretching region (2970–2850 cm^{-1}) could be an indication of oxygenated compounds adsorbed on both catalysts.

To determine if the features shown in Fig. 8b could be related to ethanol, ethanol exposure was carried out on the promoted catalyst. Fig. 9 shows the FTIR spectrum of pre-reduced Rh–Li/TiO_2

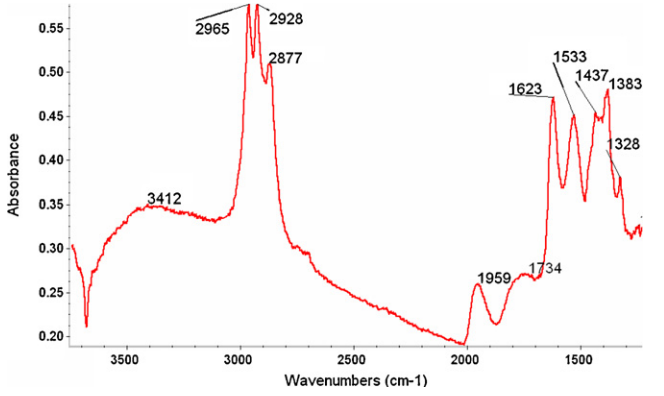

Fig. 9. FTIR spectrum recorded during ethanol adsorption and decomposition at 270 °C over the pre-reduced Rh–Li/TiO_2.

under ethanol flow at reaction temperature. The observed C–H vibrations and low wave number modes (1200–1700 cm^{-1}) resulting from ethanol adsorption or decomposition can be clearly identified and match well with the species seen in Fig. 8b. The peaks related to C–H stretching vibrations, and possibly oxygenated intermediates, are slightly more pronounced in the case of promoted Rh–Li/TiO_2 (Fig. 8b), corroborating reaction tests that show improved selectivity for oxygenated compounds in the case of Li-promoted catalyst.

4. Conclusions

1. Li enhances the dispersion of Rh, reducing the formation of large Rh atom ensembles on the surface that is required for the CO dissociation. Less CO dissociation is thought to reduce surface carbon coverage leading to increased H_2 chemisorption which is necessary for improved activity and selectivity to ethanol [33].
2. Li makes Rh less reducible thereby increasing CO insertion which is thought to require oxidized Rh.
3. Li promotion leads to more reactive adsorbed CO species, increasing CO conversion.
4. The presence of the Li promoter does not seem to alter the electronic structure of Rh, but rather it can introduce structural changes that could alter the Rh dispersion and the bonding of CO on Rh or at its support interface.
5. Under temperature and a gas mixture that mimic reaction conditions, there is no evidence of cationic Rh since gem-dicarbonyl species are not observed in either Rh or Rh–Li supported catalyst.

Acknowledgements

This work was supported by the U.S. Department of Energy/National Engineering Technology Lab. (contract no: DE-FC26-06NT43024, Project Officer: Dan Driscoll). Reaction studies, TPD and TPR were carried out at Louisiana State University and at FTIR experiments were carried out at Oak Ridge National Laboratory's Center for Nanophase Materials Sciences, which is sponsored by the DOE BES Office of Scientific Facilities. The authors wish to thank Karren Moore and Shawn Reeves at ORNL's High Temperature Materials Laboratory for microscopy and analysis.

References

[1] H. Arakawa, T. Fukushima, M. Ichikawa, S. Natsushita, K. Takeuchi, T. Matsuzaki, Y. Sugi, Chemistry Letters (1985) 881–884.
[2] M.M. Bhasin, W.J. Bartley, P.C. Ellgen, T.P. Wilson, Journal of Catalysis 54 (1978) 120–128.
[3] H. Ehwald, H. Ewald, D. Gutschick, M. Hermann, H. Miessner, G. Öhlmann, E. Schierhorn, Applied Catalysis 76 (1991) 153–169.
[4] R. Burch, M.I. Petch, Applied Catalysis A: General 88 (1992) 39–60.
[5] H.M. Yin, Y.J. Ding, H.Y. Luo, H.J. Zhu, D.P. He, J.M. Xiong, L.W. Lin, Applied Catalysis A: General 243 (2003) 155–164.
[6] P. Forzatti, E. Tronconi, I. Pasquon, Catalysis Reviews: Science and Engineering 33 (1991) 109–168.
[7] J.J. Spivey, A.A. Egbebi, Chemical Society Reviews 36 (2007) 1514–1528.
[8] B.J. Kip, E.G.F. Hermans, R. Prins, Applied Catalysis 35 (1987) 141–152.
[9] S.C. Chuang, J.G. Goodwin, I. Wender, Journal of Catalysis 95 (1985) 435–446.
[10] S.S.C. Chuang, R.W. Stevens, R. Khatri, Topics in Catalysis 32 (2005) 225–232.
[11] H. Kusama, K. Okabe, K. Sayama, H. Arakawa, Catalysis Today 28 (1996) 261–266.
[12] S.C. Chuang, J.G. Goodwin, I. Wender, Journal of Catalysis 92 (1985) 416–421.
[13] H. Kato, M. Nakashima, Y. Mori, T. Mori, T. Hattori, Y. Murakami, Research on Chemical Intermediates 21 (1995) 115–126.
[14] H.Y. Luo, W. Zhang, H.W. Zhou, S.Y. Huang, P.Z. Lin, Y.J. Ding, L.W. Lin, Applied, Catalysis A: General 214 (2001) 161–166.
[15] M. Ichikawa, T. Fukushima, Journal of the Chemical Society: Chemical Communications (1985) 321–323.
[16] H.M. Yin, Y.J. Ding, H.Y. Luo, D.P. He, W.M. Chen, Z.Y. Ao, L.W. Lin, Journal of Natural Gas Chemistry 12 (2003) 233–236.
[17] R. Burch, M.J. Hayes, Journal of Catalysis 165 (1997) 249–261.

[18] M. Ojeda, M.L. Granados, S. Rojas, P. Terreros, F.J. Garcia-Garcia, J.L.G. Fierro, Applied Catalysis A: General 261 (2004) 47–55.
[19] M.P. Cabero, M.J. Holgado, V. Rives, Materials Chemistry and Physics 27 (1991) 181–188.
[20] U. Usman, M. Takaki, T. Kubota, Y. Okamoto, Applied Catalysis A: General 286 (2005) 148–154.
[21] I.E. Wachs, G. Deo, M.A. Vuurman, H.C. Hu, D.S. Kim, J.M. Jehng, Journal of Molecular Catalysis 82 (1993) 443–455.
[22] T. Ioannides, X. Verykios, Journal of Catalysis 140 (1993) 353–369.
[23] C. Wong, R.W. McCabe, Journal of Catalysis 107 (1987) 535–547.
[24] R.P. Underwood, A.T. Bell, Journal of Catalysis 109 (1988) 61–75.
[25] P. Basu, D. Panayotov, J.T. Yates, Journal of the American Chemical Society 110 (1988) 2074–2081.
[26] C.A. Rice, S.D. Worley, C.W. Curtis, J.A. Guin, A.R. Tarrer, Journal of Chemical Physics 74 (1981) 6487–6497.
[27] I.A. Fisher, A.T. Bell, Journal of Catalysis 162 (1996) 54–65.
[28] H. Kusama, K. Sayama, K. Okabe, H. Arakawa, Nippon Kagaku Kaishi (1995) 875–880.
[29] J.A. Chudek, M.W. Mcquire, G.W. Mcquire, C.H. Rochester, Journal of the Chemical Society: Faraday Transactions 90 (1994) 3699–3709.
[30] G. Busca, H. Saussey, O. Saur, J.C. Lavalley, V. Lorenzelli, Applied Catalysis 14 (1985) 245–260.
[31] T. Iwasita, E. Pastor, Electrochimica Acta 39 (1994) 531–537.
[32] T. Fukushima, H. Arakawa, M. Ichikawa, Journal of Physical Chemistry 89 (1985) 4440–4443.
[33] R. Burch, M.I. Petch, Applied Catalysis A: General 88 (1992) 77–99.